Earth Planets Space, **62**, 843–848, 2010

Solar cycle dependence of quiet-time magnetospheric currents and a model of their near-Earth magnetic fields

Hermann Lühr[1] and Stefan Maus[2,3]

[1]*GFZ, German Research Centre for Geoscience, Potsdam, Germany*
[2]*Cooperative Institute for Research in Environmental Sciences—CIRES, Boulder, USA*
[3]*National Geophysical Data Center—NGDC/NOAA, Boulder, USA*

(Received April 27, 2010; Revised July 7, 2010; Accepted July 20, 2010; Online published December 31, 2010)

Satellite measurements from high-resolution magnetic field mapping missions over almost a complete solar cycle have been used to investigate the variability of major magnetospheric currents during quiet times. As judged from near-Earth magnetic field observations, the magnetotail current system exhibits no long-term trend. Activity-dependent enhancements decay within hours. A suitable quantity to parameterize the temporal variation is the merging electric field, delayed by 60 minutes with respect to its value at the bow shock. Conversely, the ring current strength shows pronounced solar cycle dependences. We show for the first time that a solar cycle dependent bias has to be added to D_{ST} to represent the actual ring current strength. It ranges from -15 nT at solar maximum to zero at solar minimum. The scaled solar flux index, $F_{10.7}$, delayed by 20 months, is found to be a suitable proxy for predicting the bias. This empirical result reflects no physical relation between $F_{10.7}$ and ring current bias. A spherical harmonic model valid at Earth's surface is presented that reflects the quiet-time magnetospheric fields.

Key words: Geomagnetism, magnetic field modelling, magnetospheric fields, magnetospheric currents.

1. Introduction

For high-resolution geomagnetic field modeling from data of low-Earth orbiting satellites, uncertainties in characterizing contributions from ionospheric and magnetospheric currents can be regarded as the prime limiting factor for the achievable accuracy. For satellites, the ionospheric currents generally represent internal sources. Large-scale magnetospheric currents flow on the magnetopause. They include the Chapman-Ferraro (CF) currents on the sunward side, and they are part of the magnetotail current system on the night side (e.g., Hughes, 1995). Furthermore a magnetospheric ring current circles the Earth, aligned with the geomagnetic equatorial plane. Large-scale field-aligned currents connect the various magnetospheric currents with the high-latitude ionosphere (e.g., McPherron, 1995).

If vector field measurements are available over the complete surface of a sphere, then it is possible to uniquely distinguish between (1) internal poloidal fields from sources below the satellite (e.g. core, crust, E-region currents), (2) toroidal fields due to field-aligned currents passing through the orbital plane, and (3) poloidal fields flowing entirely above the satellite orbit (e.g. magnetospheric currents). We make use of this important property of spherical harmonic (SH) analysis to derive a model of the external poloidal field, which reflects typical characteristics of magnetospheric current systems. Our analysis is limited to quiet times ($K_p < 3$) because of their relevance for modeling Earth's internal magnetic field.

It has been recognized for quite some time that currents in the inner magnetosphere (i.e. the ring current) are well described in the solar-magnetic (SM) frame. In that frame the z axis is parallel to the geomagnetic dipole axis, pointing northward, the y axis is perpendicular to the plane defined by dipole axis and the Sun-Earth line, points toward dusk and x completes the triad pointing sunward. Currents in the outer magnetosphere are better organized in geocentric-solar-magnetospheric (GSM) coordinates. In that case the x axis points to the sun, the y axis is perpendicular to the plane defined by the x axis and the dipole axis, pointing duskward, and z completes the triad, pointing northward. For an efficient description of the external magnetic features it has recently been proposed to separately expand the contributions in SM and GSM coordinates (Maus and Lühr, 2005; Olsen *et al.*, 2005). A reliable separation between field variations in the GSM and SM frames is not simple but, it is achievable. The orientation of the two frames differs by up to $\pm 34^\circ$ during the solstice seasons. For a reliable separation, at least one year of data has to be analyzed.

A basic SH model of the near-Earth external magnetic field was compiled by Maus and Lühr (2005) (hereafter referred to as ML (2005)), making use of Ørsted and CHAMP data of the years 2000–2004. It may be noted that the external SH coefficient of degree $n = 1$ and order $m = 0$ (subsequently termed coeff $(1, 0)$) describes a uniform field anti-parallel to the z axis of the coordinate system. The geometries of higher degree terms are described elsewhere (e.g. Langel, 1987). The salient features of that model are

doi:10.5047/eps.2010.07.012

1) a constant field (coeff (1, 0)) in GSM coordinates of about 13 nT pointing in opposite direction to the Z_{GSM} component,
2) a field contribution in the Y_{GSM} direction that varies at a quarter of the strength of the interplanetary magnetic field (IMF) B_y component,
3) a constant field (coeff (1, 0)) in SM coordinates of about 7.6 nT pointing in opposite direction to the Z_{SM} component,
4) a field component along the Z_{SM} axis varying as $0.8 \cdot E_{ST}$, the external part of the D_{ST} index.

In addition, all the magnetic effects due to induction in the Earth have been considered. Presently this kind of parameterization is widely accepted in the main field modeling community, and it is employed, for example, in model families such as CHAOS (CHAMP, Ørsted, SAC-C) (e.g., Olsen *et al*., 2006) and Pomme (e.g., Maus *et al*., 2006).

In recent years it has become increasingly evident that the model of ML (2005) has to be updated in order to better represent the present magnetospheric field under solar minimum conditions. It has been suggested that the constant terms in items 1 and 3 (above) may show some secular variation. In this study we make use of 9 years of CHAMP magnetic field measurements to check the time dependence of the magnetospheric contributions. In the second step suitable proxies are investigated that can be used for parameterizing the temporal changes of the magnetospheric fields.

2. Data Set and Processing Approach

Prime data sources for this study are the CHAMP vector and scalar magnetic field measurements. They are fully calibrated and available under product identifier CH-ME-2-FGM-NEC and CH-ME-2-OVM, respectively, from the Information and Science Data Center (ISDC) at GFZ in Potsdam. The employed data interval starts immediately following the launch of CHAMP, 15 July 2000, and lasts until the end of August 2009. Therefore the entire time span, from the peak of the solar cycle to the present deep minimum, is covered. Ørsted data are used for validation purposes. Magnetic field vector data are considered from July 2000 until November 2005 sampled by that spacecraft. Since vector data become progressively sparse after July 2002, Ørsted scalar data from July 2002 to June 2009 are also taken into account.

For main field modeling, data is commonly selected from periods of low magnetic activity. We therefore exclude storm times from our study. Data were selected from periods when the magnetic activity index, a_m, was less than 15 ($K_p < 3$) and the previous 3-hour interval had $a_m < 18$. Rapid variations of magnetospheric currents on time scales of the orbital period (1.5 h) are excluded from such a dataset. Furthermore, data from orbits showing abnormal signatures were discarded. No selection with respect to solar wind, IMF or D_{ST} conditions was performed. The index a_m is an alternative version of a_p (for details see Menvielle and Marchaudon (2007)).

Before interpreting the effects of magnetospheric currents, we subtracted all other known field contributions. The main field is removed by means of the Pomme-5 model, which is very similar to Pomme-6 (Maus *et al*., 2010). Ionospheric currents in the F region driven by plasma pressure gradients are corrected for, as proposed by Lühr *et al*. (2003), making use of the electron density and temperature measurements of CHAMP and an estimate of the ion temperature, T_i, following Köhnlein (1986)

$$T_i = 900 + 200 \cos\left\{\frac{\pi}{12}(\mathrm{LT} - 14)\right\} \quad (1)$$

where the resulting temperature is in Kelvin (K) and LT represents the local time in hours.

To estimate the coefficients describing the magnetospheric field, we make use of a spherical harmonic expansion by solving simultaneously for coefficients in the GSM and SM frames. Since satellites sample the sphere more densely near the poles than at the equator, an equal-area data weighting is performed prior to the least-squares inversion. Subsequently we make use of the SHA property to derive the coefficients of an external poloidal field.

3. Results

The magnetospheric field model derived from CHAMP data has the same structure as the one presented by ML (2005). Due to the longer data interval, time dependences can be investigated. We have used two different approaches to describe the temporal variation of the external field. First we derived the mean magnetospheric contribution from an independent inversion for every year. Subsequently we fitted all data in a single run, accounting for temporal variations over the 9 years by an appropriate parameterization.

3.1 Temporal variations of the GSM and SM fields

One prominent result of ML (2005) was the identification of a stable coeff (1, 0) magnetic field of about 13 nT in the GSM frame. When considering the full span of 9 years of continuous CHAMP recordings, it becomes evident that the GSM field shows no solar cycle dependence. Figure 1 displays the yearly results. The crosses with uncertainty bars represent the annual means of the negative Z_{GSM} component. They vary around 8.5 nT without exhibiting any trend.

Simultaneously, the annual means of the external field (coeff (1, 0)) aligned with the negative Z_{SM} component are calculated. Results are presented in Fig. 2 as plus signs with error bars. This quantity shows major solar cycle dependence. Large annual means up to 17 nT are obtained during the years 2001 through 2005; subsequently they decay to 2 nT in 2009. An interpretation in terms of magnetospheric currents will be given in Section 4.

3.2 Modeling of the external fields

A widely accepted approach is the parameterization of the various external field sources by suitable parameters. In the case of the SM field, Maus and Weidelt (2004) proposed the E_{ST} index (external part of D_{ST}) as a suitable proxy for describing the temporal changes of the ring current effect. In addition, a bias value has to be considered, reflecting the magnetic effect of the quiet-time ring current (for $E_{ST} = 0$). The annual means shown in Fig. 2 suggest that the bias can no longer be considered as constant when analyzing a 9-year interval.

In order to obtain a continuous description of the near-

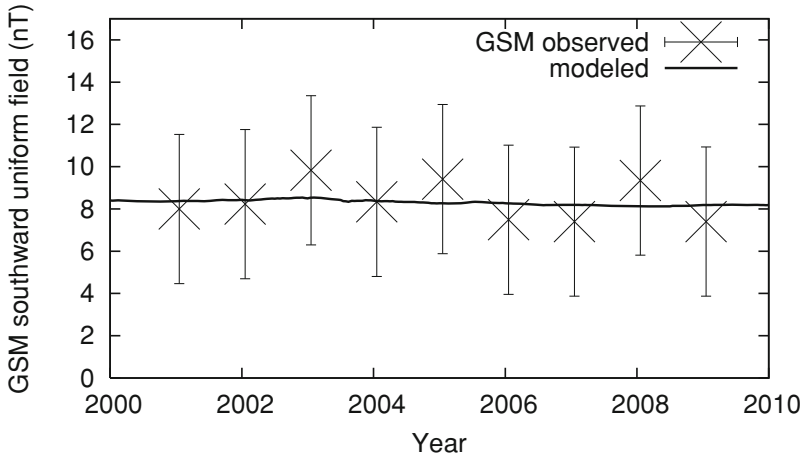

Fig. 1. Long-term variation of magnetospheric field component in GSM coordinates. Annual means of the $-Z_{\mathrm{GSM}}$ component as derived from CHAMP data (crosses); model prediction of the $-Z_{\mathrm{GSM}}$ component (full line). Error bars reflect the RMS difference between CHAMP and Ørsted annual means.

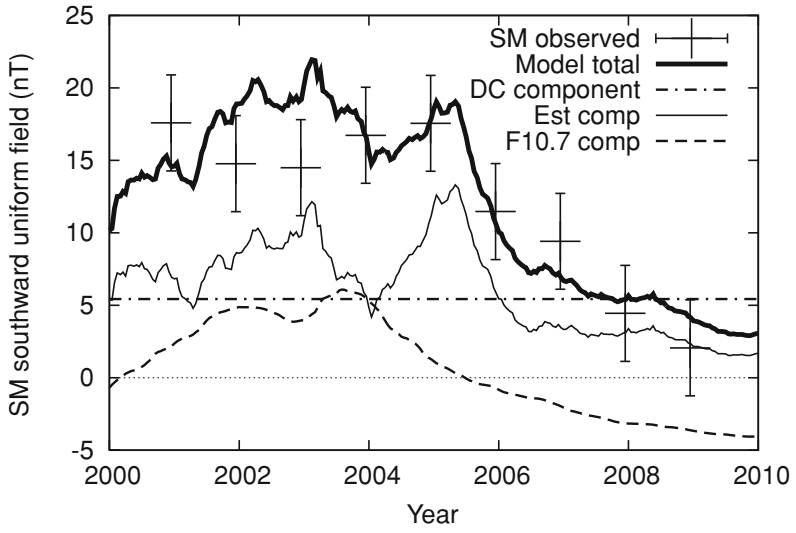

Fig. 2. Breakdown of the parts contributing to the uniform field in SM coordinates. The observed annual mean values of SM fields are presented as plus signs. The model estimate of the $-Z_{\mathrm{SM}}$ component is drawn as thick curve. This is composed of a constant bias (dashed-dotted), an E_{ST} dependent component (thin line), and a solar cycle dependent component approximated by the $F_{10.7}$ index delayed by 20 months (dashed).

Earth external field, we have introduced a number of controlling parameters for the SM and GSM models. Scaling and temporal shift of these parameters are optimized by minimizing the difference between model prediction and satellite observations. The SM model (mainly coeff (1, 0)) is controlled by three different entries. Time variations (order of days) are accounted for by a parameterization with the E_{ST} index. The strength and variation of the E_{ST}-related part is plotted in Fig. 2 as a thin line. This curve is systematically below the annual means. To reconcile the model with the observations, we tested several solar cycle dependent functions that could represent the time-variable bias. Promising results were obtained using the solar flux ($F_{10.7}$ index) delayed by about 20 months, for parameterizing the second part (dashed curve). The third part is a constant bias (dashed-dotted curve).

The attained match between SM field model (heavy line) and observation (plus signs) is shown in Fig. 2. The most appropriate delay time for the 81-day running mean of $F_{10.7}$ (termed $F_{10.7\mathrm{a}}$) has been determined empirically by testing the RMS discrepancy between model prediction and observation. As can be seen from Fig. 3 (top frame), best results are achieved when the field lags behind $F_{10.7\mathrm{a}}$ by 18–22 months. We obtain consistent delay times from independently processed CHAMP and Ørsted data. For our final model we selected a time lag of 20 months, to be applied to the $F_{10.7\mathrm{a}}$ readings. Taking all these effects into account, the SM field in nT is modeled (coeff (1, 0)) as

$$Z_{\mathrm{SM}} = -[5.43 + 0.080(F_{10.7\mathrm{a}_{\mathrm{lag}}} - 120) - 0.87E_{\mathrm{ST}}] \quad (2)$$

where the solar flux values have been centered about their mean value, $F_{10.7} = 120$ sfu.

We also modeled the external field part in the GSM frame. Although no long-term trend emerged from the annual means in Fig. 1, improvements on shorter time scales have been tested. The GSM field has been related to currents in the outer magnetosphere. The strength of the transpolar cap potential may be regarded as a suitable indicator

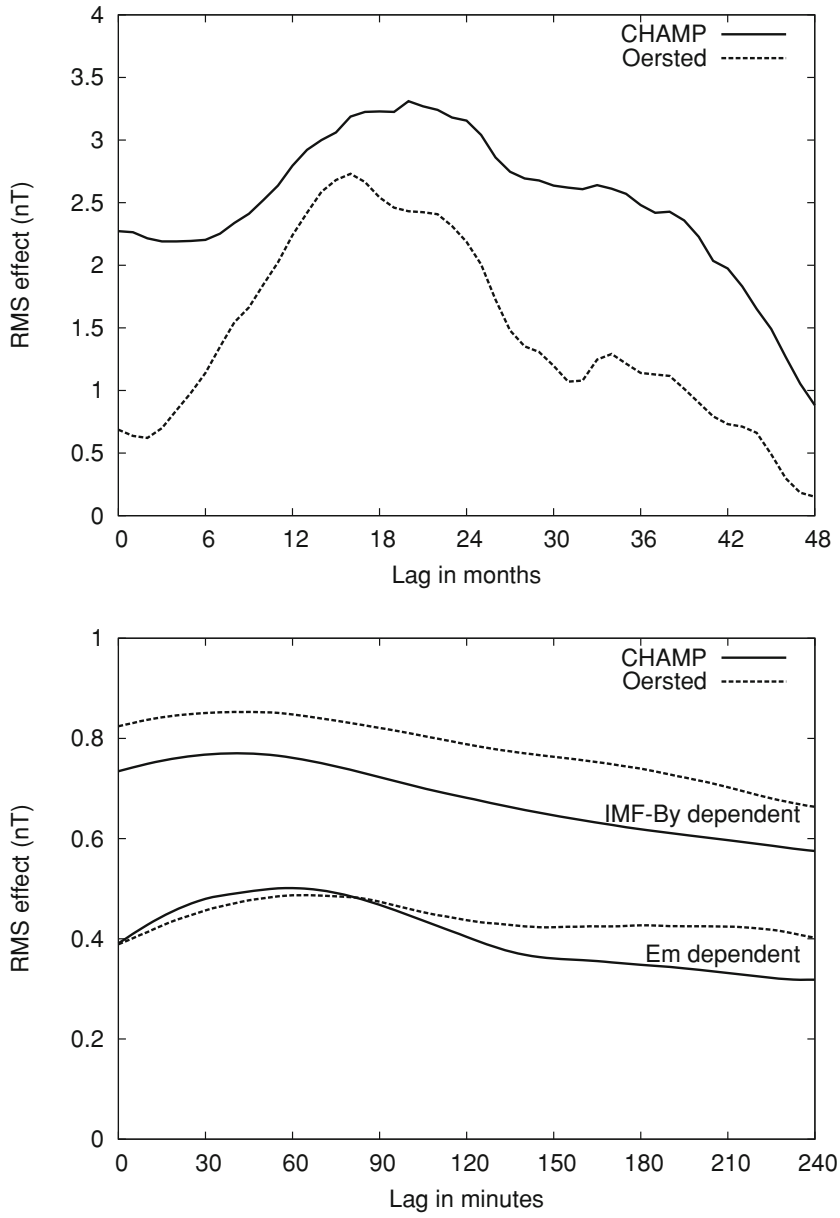

Fig. 3. Determination of optimal lag time by plotting the root mean square (RMS) of the effect that can be explained by the model. (*top frame*) The $F_{10.7}$ index is used as a proxy for the bias of the uniform SM field. Best results are obtained when the $F_{10.7}$ index is delayed by 18 to 22 months. (*bottom frame*) The model parameterization is optimal when IMF B_y is delayed by 35 min and the merging electric field, E_m, by 60 min with respect to IMF observations at the bow shock.

for magnetospheric convection. Since there is no dedicated index representing this potential, we make use of its linear correlation with the merging electric field, E_m, as suggested by Kan and Lee (1979). According to these authors E_m is calculated as

$$E_\mathrm{m} = v_\mathrm{SW} \left(B_y^2 + B_z^2\right)^{\frac{1}{2}} \sin^2\left(\frac{\Theta}{2}\right) \tag{3}$$

where v_SW is solar wind velocity, B_y and B_z are IMF components in GSM frame and Θ is the clock angle of the IMF. For strong solar wind conditions, the transpolar potential goes into saturation. Ober *et al*. (2003) derived saturation curves for the transpolar potential from DMSP measurements. We make use of their results for computing an effective electric field, E'_m

$$E'_\mathrm{m} = 8E_\mathrm{m}\left(64 + E_\mathrm{m}^2\right)^{-0.5} \tag{4}$$

where E_m is in mV/m.

The parameterization of the GSM model by E_m was validated by comparison with observations. As can be seen in Fig. 3 (bottom frame), an optimal agreement between the data sets is obtained for an E'_m delayed by 60 minutes with respect to solar wind data at the bow shock. The uniform GSM field in nT is calculated as follows

$$Z_\mathrm{GSM} = -\left[8.31 + 1.38\left(E'_\mathrm{m} - 0.5\right)\right] \tag{5}$$

where E'_m is in mV/m. The temporal evolution of the modeled GSM coeff $(1, 0)$ is plotted in Fig. 1 as a full line. No trend emerges.

Table 1. List of external SHA coefficients (in nT) for modeling the near-Earth magnetospheric field. Coefficients derived independently from Ørsted data are shown for comparison.

Frame	Contribution		CHAMP					Ørsted				
			Order m					Order m				
		n	0	1	−1	2	−2	0	1	−1	2	−2
SM	Stable field	1	5.43					5.59				
		2		−0.95	0.90				−0.68	1.16		
	$a = (F_{10.7} - 120)$	1	$0.080 \cdot a$					0.059				
		2		$-0.002 \cdot a$	$0.000 \cdot a$				−0.009	0.002		
	E_{ST}/I_{ST}	1	$0.87 \cdot E_{ST}$					0.84				
GSM	Stable field	1	8.31	0.09	0.43			9.34	0.20	0.65		
		2	0.13	−0.68	−1.29	0.00	0.52	−0.10	−0.90	−1.02	−0.07	0.66
	$b = \mathrm{IMF}B_y$	1		$0.07 \cdot b$	$-0.26 \cdot b$				0.11	−0.27		
	$c = (E_m - 0.5)$	1	$1.38 \cdot c$					1.35				

In this study we also confirm the partial penetration of the IMF B_y field to the Earth's surface. The scaling factor 0.26 confirms earlier results (e.g., Lesur *et al*. (2005); ML (2005)). A new element is the optimal delay of 35 minutes with respect to the IMF reading at the bow shock (see Fig. 3, bottom).

This new parameterization allows the external field contribution to be modeled more reliably over long periods. Details of the SHA coefficients used in this model are compiled in Table 1. For comparison, the most appropriate coefficients derived from independent Ørsted data are added. In general, the coefficients from both satellites and both orbital altitudes agree reasonably well, supporting the reliability of our model. We believe that the CHAMP observations are more suitable for separating the fields in SM and GSM frames, partly because of differences in orbital dynamics. It takes Ørsted almost 4.5 years to precess through all local times, compared to only 261 days in the case of CHAMP.

4. Discussion and Conclusion

The evaluation of continuous magnetic field recordings from satellite over 9 years has revealed new features of magnetospheric field contributions. These features are of concern for main field modelers. In this section we interpret the modeled magnetic fields in terms of currents. In ML (2005), variations in GSM coordinates had been related to the far-field effect of the tail lobe field, and field contributions in the SM frame were related to the ring current plus the Chapman-Ferraro currents.

An important result is the time-dependent bias of the D_{ST} (E_{ST}) index. This means that the D_{ST} value underestimates the actual field produced by the ring current by a varying amount, ranging from 0 to 15 nT depending on solar cycle phase. The observatory baseline, which is used for D_{ST} estimation, is obviously contaminated by the slowly varying quiet-time ring current field. Previous modeling studies based on observatory data may have suffered from this imperfection. According to the Dressler-Parker-Schopke theorem, the total energy of the particles in the ring current is proportional to the magnetic field effect at the Earth's surface. According to Eq. (2), at very low solar flux (e.g. $F_{10.7a} = 60$) and vanishing E_{ST} (D_{ST}) value the ring current practically disappears. Satellite missions such as Cluster and/or THEMIS should be used to verify the ring current decay during this deep solar minimum.

To parameterize the solar cycle dependence of the E_{ST} (D_{ST}) bias, the solar flux index $F_{10.7a}$ was used here. No direct causal dependence between the two quantities exists. Therefore, $F_{10.7a}$ is probably not the most suitable choice. Significant differences between the observations and the model curve (heavy line in Fig. 1) appear for the years 2002 and 2003. The obtained relationship is probably only valid for solar cycle 23. Thus, the search for a more appropriate parameter reflecting the quiet-time ring current field should be continued.

Another important finding of this study is the long-term stability of the contribution in GSM coordinates. Variations of the field strength aligned with the Z_{GSM} component occur on time scales of hours. We identified the merging electric field as a suitable parameter for describing the short-term variability outside of magnetic storms. The derived time-delay for E_m of 60 minutes with respect to conditions at the bow shock, when parameterizing the Z_{GSM} field variations, supports the suggestion of ML (2005), namely, that the field in the GSM frame is primarily caused by tail currents. This implies that no solar cycle dependence of the average tail lobe field could be deduced. The magnetic field generated by Champman-Ferraro currents likely ends up as part of the SM component.

From Eq. (5) we see that close to Earth a GSM field of 8.3 nT is found for $E_m = 0.5$ mV/m. This result is smaller than the stable GSM value of 12.9 nT mentioned by ML (2005). Part of the difference can be explained by the higher merging electric field during the years 1999–2004, but some 3 nT remain unexplained. Olsen *et al*. (2005) also presented a decomposition of the external magnetic field in SM and GSM parts. Their reported value of 8.3 nT for the GSM field agrees fully with the value presented here.

In summary, important features of magnetospheric fields, as observed close to Earth, have been inferred in this study. Solar cycle dependences of the magnetospheric ring current and tail currents were deduced. A new time-dependent SHA model characterizing the different quiet-time magnetospheric contributions has been presented and is available as part of the software of the Pomme-6 model at http://geomag.org/models/pomme6.html. The European

Space Agency's upcoming multi-satellite mission Swarm should be used to develop improved magnetospheric current indices, complementing D_{ST}.

Acknowledgments. The CHAMP mission is sponsored by the Space Agency of the German Aerospace Center (DLR) through funds of the Federal Ministry of Economics and Technology, following a decision of the German Federal Parliament (grant code 50EE0944). The data retrieval and operation of the CHAMP satellite by the German Space Operations Center (GSOC) is acknowledged. The Ørsted Project was made possible by extensive support from the Danish Government, NASA, ESA, CNES and DARA.

References

Hughes, W. J., The magnetopause, magnetotail, and magnetic reconnection, in *Introduction to Space Physics*, edited by M. G. Kivelson and C. T. Russell, 227–287, Cambridge University Press, 1995.

Kan, J. R. and L. C. Lee, Energy coupling function and solar wind magnetosphere dynamo, *Geophys. Res. Lett.*, **6**, 577–580, 1979.

Köhnlein, W., A model of the electron and ion temperatures in the ionosphere, *Planet. Space Sci.*, **34**, 609–630, 1986.

Langel, R., The main field, in *Geomagnetism*, edited by J. A. Jacobs, vol. 1, 249–512, Academic Press, Orlando, 1987.

Lesur, V., S. Macmillan, and A. Thomson, A magnetic field model with daily variations of the magnetospheric field and its induced counterpart in 2001, *Geophys. J. Int.*, **160**, 79–88, 2005.

Lühr, H., M. Rother, S. Maus, W. Mai, and D. Cooke, The diamagnetic effect of the equatorial Appleton anomaly: Its characteristics and impact on geomagnetic field modelling, *Geophys. Res. Lett.*, **30**(17), 1906, doi:10.1029/2003GL017407, 2003.

Maus, S. and H. Lühr, Signature of the quiet-time magnetospheric magnetic field and its electromagnetic induction in the rotating Earth, *Geophys. J. Int.*, **162**, 755–763, doi:10:1111/j.1365-246X.2005.02691.x, 2005.

Maus, S. and P. Weidelt, Separating the magnetospheric disturbance magnetic field into external and transient internal contributions using a 1D conductivity model of the earth, *Geophys. Res. Lett.*, **31**, L12614, doi:10.1029/2004GL020232, 2004.

Maus, S., M. Rother, C. Stolle, W. Mai, S.-C. Choi, H. Lühr, D. Cooke, and C. Roth, Third generation of the Potsdam Magnetic Model of the Earth (POMME), *Geochem. Geophys. Geosyst.*, **7**, Q07008, doi:10.1029GC001269, 2006.

Maus, S., C. Manoj, J. Rauberg, I. Michaelis, and H. Lühr, NOAA/NGDC candidate models for the 11th generation International Geomagnetic Reference Field and the concurrent release of the 6th generation Pomme magnetic model, *Earth Planets Space*, **62**, this issue, 729–735, 2010.

McPherron, R. L., Magnetospheric dynamics, in *Introduction to Space Physics*, edited by M. G. Kivelson and C. T. Russell, 400–458, Cambridge University Press, 1995.

Menvielle, M. and A. Marchaudon, Geomagnetic indices in solar-terrestrial physics and space weather, Space Weather, research toward applications in Europe, in *Astrophysics and Space Science Library*, edited by J. Lilensten, p 277–288, Springer, Berlin-Heidelberg, 2007.

Ober, D. M., N. C. Maynard, and W. J. Burke, Testing the Hill model of transpolar potential saturation, *J. Geophys. Res.*, **108**(A12), 1467, doi:10.1029/2003JA010154, 2003.

Olsen, N., T. J. Sabaka, and F. Lowes, New parameterization of external and induced fields in geomagnetic field modeling, and a candidate model for IGRF 2005, *Earth Planets Space*, **57**, 1141–1149, 2005.

Olsen, N., H. Lühr, T. J. Sabaka, M. Mandea, M. Rother, L. Tøffner-Clausen, and S. Choi, CHAOS—A model of the Earth's magnetic field derived from CHAMP, Ørsted, and SAC-C magnetic satellite data, *Geophys. J. Int.*, 67–75, doi:10.1111/j.1365-246X.2006.02959, 2006.

H. Lühr (e-mail: hluehr@gfz-potsdam.de) and S. Maus